HAL
open science

The Budyko functions under non-steady-state conditions

Roger Moussa, Jean-Paul Lhomme

To cite this version:

Roger Moussa, Jean-Paul Lhomme. The Budyko functions under non-steady-state conditions. Hydrology and Earth System Sciences, 2016, 20 (12), pp.4867-4879. 10.5194/hess-20-4867-2016 . hal-01602425

HAL Id: hal-01602425

https://hal.science/hal-01602425v1

Submitted on 27 May 2020

HAL is a multi-disciplinary open access archive for the deposit and dissemination of scientific research documents, whether they are published or not. The documents may come from teaching and research institutions in France or abroad, or from public or private research centers.

L'archive ouverte pluridisciplinaire **HAL**, est destinée au dépôt et à la diffusion de documents scientifiques de niveau recherche, publiés ou non, émanant des établissements d'enseignement et de recherche français ou étrangers, des laboratoires publics ou privés.

Distributed under a Creative Commons Attribution 4.0 International License

Hydrol. Earth Syst. Sci., 20, 4867–4879, 2016
www.hydrol-earth-syst-sci.net/20/4867/2016/
doi:10.5194/hess-20-4867-2016
© Author(s) 2016. CC Attribution 3.0 License.

Hydrology and Earth System Sciences
Open Access

The Budyko functions under non-steady-state conditions

Roger Moussa[1] **and Jean-Paul Lhomme**[2]

[1]INRA, UMR LISAH, 2 place Viala, 34060 Montpellier, France
[2]IRD, UMR LISAH, 2 place Viala, 34060 Montpellier, France

Correspondence to: Roger Moussa (roger.moussa@inra.fr)

Received: 22 July 2016 – Published in Hydrol. Earth Syst. Sci. Discuss.: 26 July 2016
Revised: 19 October 2016 – Accepted: 16 November 2016 – Published: 12 December 2016

Abstract. The Budyko functions relate the evaporation ratio E / P (E is evaporation and P precipitation) to the aridity index $\Phi = E_p / P$ (E_p is potential evaporation) and are valid on long timescales under steady-state conditions. A new physically based formulation (noted as Moussa–Lhomme, ML) is proposed to extend the Budyko framework under non-steady-state conditions taking into account the change in terrestrial water storage ΔS. The variation in storage amount ΔS is taken as negative when withdrawn from the area at stake and used for evaporation and positive otherwise, when removed from the precipitation and stored in the area. The ML formulation introduces a dimensionless parameter $H_E = -\Delta S / E_p$ and can be applied with any Budyko function. It represents a generic framework, easy to use at various time steps (year, season or month), with the only data required being E_p, P and ΔS. For the particular case where the Fu–Zhang equation is used, the ML formulation with $\Delta S \leq 0$ is similar to the analytical solution of Greve et al. (2016) in the standard Budyko space (E_p / P, E / P), a simple relationship existing between their respective parameters. The ML formulation is extended to the space $[E_p / (P - \Delta S),\ E / (P - \Delta S)]$ and compared to the formulations of Chen et al. (2013) and Du et al. (2016). The ML (or Greve et al., 2016) feasible domain has a similar upper limit to that of Chen et al. (2013) and Du et al. (2016), but its lower boundary is different. Moreover, the domain of variation of $E_p / (P - \Delta S)$ differs: for $\Delta S \leq 0$, it is bounded by an upper limit $1 / H_E$ in the ML formulation, while it is only bounded by a lower limit in Chen et al.'s (2013) and Du et al.'s (2016) formulations. The ML formulation can also be conducted using the dimensionless parameter $H_P = -\Delta S / P$ instead of H_E, which yields another form of the equations.

1 Introduction

The Budyko framework has become a simple tool that is widely used within the hydrological community to estimate the evaporation ratio E / P at catchment scale (E is evaporation and P precipitation) as a function of the aridity index $\Phi = E_p / P$ (E_p is potential evaporation) through simple mathematical formulations $E / P = B_1(\Phi)$ and with long-term averages of the variables. Most of the formulations were empirically obtained (e.g., Oldekop, 1911; Turc, 1954; Tixeront, 1964; Budyko, 1974; Choudhury, 1999; Zhang et al., 2001; Zhou et al., 2015), but some of them were analytically derived from simple physical assumptions (Table 1): (i) the one derived by Mezentsev (1955) and then by Yang et al. (2008), which has the same form as the one initially proposed by Turc (1954) (noted hereafter as Turc–Mezentsev); (ii) the one derived by Fu (1981) and reworked by Zhang et al. (2004) (noted hereafter as Fu–Zhang). These two last formulations involve a shape parameter (respectively, λ and ω), which varies with catchment characteristics and vegetation dynamics (Donohue et al., 2007; Yang et al., 2009; Li et al., 2013; Carmona et al., 2014). When its value increases, actual evaporation gets closer to its maximum rate.

The Budyko framework was initially limited to steady-state conditions on long timescales, under the assumption of negligible change in soil water storage and groundwater. Hydrological processes leading to changes in water storage are not represented and the catchment is considered closed without any anthropogenic intervention: precipitation is the only input and evaporation and runoff Q the only outputs ($P = E + Q$). Recently, the Budyko framework has been downscaled to the year (Istanbulluoglu et al., 2012; Wang, 2012; Carmona et al., 2014; Du et al., 2016), the season (Gentine et al., 2012; Chen et al., 2013; Greve et al., 2016)

Table 1. Different expressions for the Budyko curves under steady-state conditions.

Reference	Equation $E / P = B_1(\Phi)$
Budyko (1974)	$\frac{E}{P} = \left\{\Phi \tanh\left(\frac{1}{\Phi}\right)\left[1-\exp(-\Phi)\right]\right\}^{1/2}$
Turc (1954) with $\lambda = 2$, Mezentsev (1955), Yang et al. (2008)	$\frac{E}{P} = \Phi\left(1+\Phi^{\lambda}\right)^{-\frac{1}{\lambda}}$
Fu (1981), Zhang et al. (2004)	$\frac{E}{P} = 1+\Phi-\left(1+\Phi^{\omega}\right)^{\frac{1}{\omega}}$
Zhang et al. (2001)	$\frac{E}{P} = \frac{1+w\Phi}{1+w\Phi+\Phi^{-1}}$
Zhou et al. (2015)	$\frac{E}{P} = \Phi\left(\frac{k}{1+k\Phi^{n}}\right)^{1/n}$

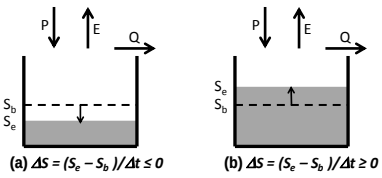

Figure 1. Representation of the change in soil water storage $\Delta S = (S_e - S_b) / \Delta t$ for the two cases considered in the paper: $\Delta S \le 0$ and $\Delta S \ge 0$. S_b and S_e are, respectively, the storage at the beginning and the end of the time period Δt.

and the month (Zhang et al., 2008; Du et al., 2016). However, the water storage variation ΔS cannot be considered as negligible when dealing with these finer timescales or for unclosed basins (e.g., soil, groundwater, reservoir, snow, interbasin water transfer, irrigation; Jaramillo and Destouni, 2015). In these cases, the catchment is considered to be under non-steady-state conditions (Fig. 1) and the basin water balance should be written as $P = E + Q + \Delta S$. Table 2 shows some recent formulations of the Budyko framework extended to take into account the change in catchment water storage ΔS. Chen et al. (2013) (used in Fang et al., 2016) and Du et al. (2016) proposed empirical modifications of the Turc–Mezentsev and Fu–Zhang equations, respectively, precipitation P being replaced by the available water supply defined as $(P - \Delta S)$, with Du et al. (2016) including the interbasin water transfer into ΔS. Greve et al. (2016) analytically modified the Fu–Zhang equation in the standard Budyko space $(E_p / P, E / P)$ introducing an additional parameter, whereas Wang and Zhou (2016) proposed in the same Budyko space a formulation issued from the hydrological ABCD model (Alley, 1984), but with two additional parameters.

With the extension of the Budyko framework to non-steady-state conditions being a real challenge, this paper aims to propose a new formulation inferred from a clear physical rationale and compared to other non-steady formulations previously derived. The paper is organized as follows. First, we present the new formulation under non-steady-state conditions: its upper and lower limits, its generic equations under restricted evaporation in the Budyko space $(E_p / P, E / P)$ and in the space $[E_p / (P - \Delta S), E / (P - \Delta S)]$. Second, we compare the new formulation to the analytical solution of Greve et al. (2016) in the standard Budyko space and to the formulations of Chen et al. (2013) and Du et al. (2016) in the space $[E_p / (P - \Delta S), E / (P - \Delta S)]$.

2 New generic formulation under non-steady-state conditions

2.1 Upper and lower limits of the Budyko framework

In the Budyko framework, each catchment is characterized by the three hydrologic variables (P, E and E_p) which are represented in a 2-D space using dimensionless variables equal to the ratio between two of these variables and the third one. In the rest of the paper, following Andréassian et al. (2016), the space defined by $(\Phi = E_p / P, E / P)$ is called Budyko space and the one defined by $(\Phi^{-1} = P / E_p, E / E_p)$ is called Turc space. For steady-state conditions $(\Delta S = 0)$, it should be recalled that any Budyko function B_1 defined in the Budyko space $(E_p / P, E / P)$ generates an equivalent function B_2 in the Turc space expressed as

$$\frac{E}{E_p} = B_2\left(\Phi^{-1}\right) = \frac{B_1(\Phi)}{\Phi}, \tag{1}$$

and that any Budyko function verifies the following conditions under steady-state conditions: (i) $E = 0$ if $P = 0$; (ii) $E \le P$ if $P \le E_p$ (water limit); (iii) $E \le E_p$ if $P \ge E_p$ (energy limit); (iv) $E \to E_p$ if $P \to \infty$.

First, we present the upper and lower limits in the Turc space under steady-state conditions, when all the water consumed by evaporation comes from the precipitation, the change in water storage ΔS being nil $(E = P - Q)$. Figure 2a represents the variation of maximum and minimum actual evapotranspiration, respectively, E_x and E_n, as a function of precipitation P with dimensionless variables. The upper solid line represents the dimensionless maximum evaporation rate E_x / E_p: it follows the precipitation up to $P / E_p = 1$ (the water limit is presented in bold blue on all graphs) and then is limited by potential evaporation $E_x / E_p = 1$ (the energy limit is in bold green). The lower solid line (in bold black) represents the dimensionless minimum evaporation rate E_n / E_p which follows the x axis: $E_n / E_p = 0$. The feasible domain between the upper and the lower limits is shown in grey. In the Budyko space, we have the following relationships: (i) when evaporation is maximum, for $E_p / P \le 1$, $E_x / P = E_p / P$ and for $E_p / P \ge 1$, $E_x / P = 1$; (ii) when evaporation is minimum: $E_n / P = 0$. The corresponding Budyko non-dimensional graph is shown in Fig. 2b and represents the upper and lower limits of the feasible domain of $E / P = B_1 (E_p / P)$.

Under non-steady-state conditions, either a given amount of water ΔS stored in the area at stake participates in the

Table 2. Different expressions for the Budyko curves under non-steady-state conditions.

Reference	Steady-state conditions $B_1(\Phi)$	Non-steady-state conditions
Greve et al. (2016)	Fu–Zhang	$\frac{E}{P} = 1 + \frac{E_p}{P} - \left[1 + (1-y_0)^{\kappa-1}\left(\frac{E_p}{P}\right)^{\kappa}\right]^{1/\kappa}$ with κ and y_0 parameters
Chen et al. (2013)	Turc–Mezentsev	$\frac{E}{P-\Delta S} = \left[1 + \left(\frac{E_p}{P-\Delta S} - \Phi_t\right)^{-\lambda}\right]^{-\frac{1}{\lambda}}$ with λ and Φ_t parameters
Du et al. (2016)	Fu–Zhang	$\frac{E}{P-\Delta S} = 1 + \frac{E_p}{P-\Delta S} - \left[1 + \left(\frac{E_p}{P-\Delta S}\right)^{\omega} + \mu\right]^{\frac{1}{\omega}}$ with ω and μ parameters

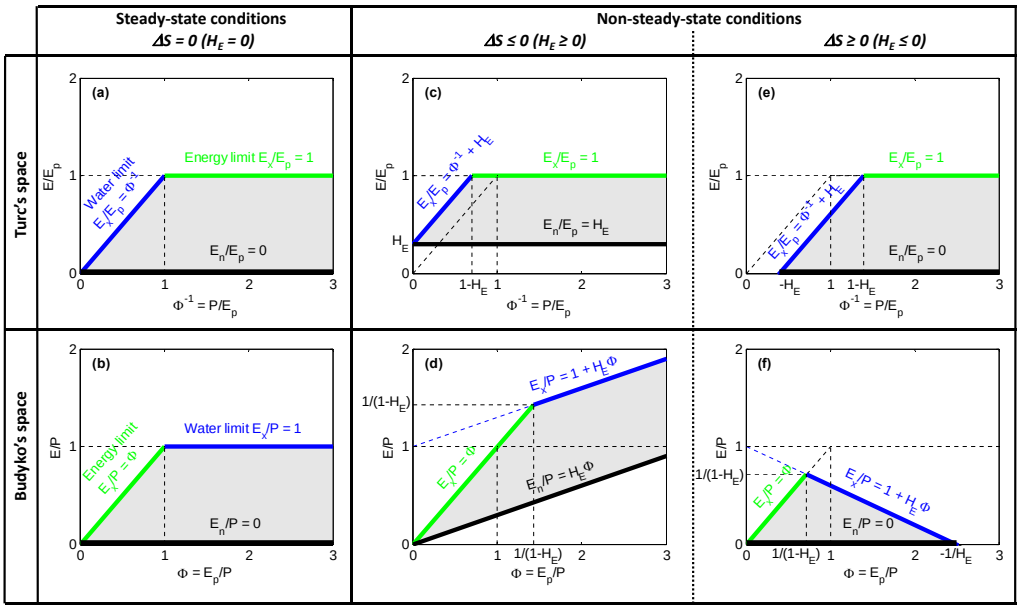

Figure 2. Upper and lower limits of the feasible domain (in grey) of evaporation in the Turc space (P / E_p, E / E_p) and in the Budyko space (E_p / P, E / P) (water limit in blue, energy limit in green and lower limit in black) when using the non-dimensional parameter H_E: (**a** and **b**) for steady-state conditions; (**c**, **d**, **e** and **f**) for non-steady-state conditions with a storage term ΔS (**c** and **d** for $\Delta S \leq 0$; and **(e)** and **(f)** for $\Delta S \geq 0$).

evaporation process (for instance, groundwater depletion for irrigation), or a given amount of the precipitation ΔS is stored in the area (soil water, ground water, reservoirs) following the water balance ($E = P - \Delta S - Q$). As shown in Fig. 1, the storage amount ΔS is taken as negative ($\Delta S \leq 0$) when withdrawn from the area and used for evaporation; it is taken as positive ($\Delta S \geq 0$) when removed from the precipitation and stored in the area. When ΔS is negative, $|\Delta S|$ should be lower than E_p because if $|\Delta S| \geq E_p$, evaporation would be systematically equal to E_p; when ΔS is positive, it should be necessarily lower than P. Consequently, $-E_p \leq \Delta S \leq P$. The variable ΔS is used in a dimensionless form, either as $H_E = -\Delta S / E_p$ or $H_P = -\Delta S / P$, which are positive when additional water is available for evapotranspiration and negative when water is withdrawn from precipitation. In the following, all the calculations are made with H_E ($-\Phi^{-1} \leq H_E \leq 1$), but a similar reasoning is conducted using H_P ($-1 \leq H_P \leq \Phi$) in Appendix A. Taking into account ΔS makes the upper and lower limits of the feasible domain different.

In the Turc space, the case where evaporation is at its maximum value is visualized as the upper limit in Fig. 2c and e (all the available water is used for evaporation). For both cases, $\Delta S \leq 0$ (Fig. 2c) or $\Delta S \geq 0$ (Fig. 2e), we have $E_x = P - \Delta S$ if $P - \Delta S \leq E_P$ and $E_x = E_P$ if $P - \Delta S \geq E_P$. Written with dimensionless variables, these equations transform into

$$\text{if } \frac{P}{E_p} \leq 1 + \frac{\Delta S}{E_p} \text{ then } \frac{E_x}{E_p} = \frac{P}{E_p} - \frac{\Delta S}{E_p} = \Phi^{-1} + H_E, \quad (2)$$

$$\text{if } \frac{P}{E_p} \geq 1 + \frac{\Delta S}{E_p} \text{ then } \frac{E_x}{E_p} = 1. \quad (3)$$

For the minimal value of evapotranspiration E_n, we have to distinguish two cases depending if $\Delta S \leq 0$ (Fig. 2c) or

$\Delta S \geq 0$ (Fig. 2e).

$$\text{if } \Delta S \leq 0 \text{ then } \frac{E_n}{E_\mathrm{p}} = \frac{-\Delta S}{E_\mathrm{p}} = H_\mathrm{E}. \tag{4a}$$

$$\text{if } \Delta S \geq 0 \text{ then } \frac{E_n}{E_\mathrm{p}} = 0 \tag{4b}$$

Translating the above equations into the Budyko space (Fig. 2d, f) yields the following for the upper limits:

$$\text{if } \frac{E_\mathrm{p}}{P} \geq \frac{E_\mathrm{p}}{E_\mathrm{p} + \Delta S} \text{ then } \frac{E_x}{P} = 1 - \frac{\Delta S}{P} = 1 + H_\mathrm{E}\frac{E_\mathrm{p}}{P} = 1 + H_\mathrm{E}\Phi, \tag{5}$$

$$\text{if } \frac{E_\mathrm{p}}{P} \leq \frac{E_\mathrm{p}}{E_\mathrm{p} + \Delta S} \text{ then } \frac{E_x}{P} = \frac{E_\mathrm{p}}{P} = \Phi. \tag{6}$$

Equation (5) has two limits: when $H_\mathrm{E} = 0$, $E_x / P = 1$, and when $\Delta S \to -E_\mathrm{p}$, which corresponds to $H_\mathrm{E} = 1$, $\mathrm{E}_x / P \to (1 + \Phi)$. For the lower limits in the Budyko space we have

$$\text{if } \Delta S \leq 0 \text{ then } \frac{E_n}{P} = \frac{-\Delta S}{P} = H_\mathrm{E}\frac{E_\mathrm{p}}{P} = H_\mathrm{E}\Phi, \tag{7a}$$

$$\text{if } \Delta S \geq 0 \text{ then } \frac{E_n}{P} = 0. \tag{7b}$$

Note that under steady-state conditions, the upper and lower limits are similar in both Turc and Budyko spaces, while this is not the case under non-steady-state conditions. It is also interesting to note that for the negative values of H_E the domain of variation of Φ is bounded $[0, -1 / H_\mathrm{E}]$ and the possible space of the Budyko functions is limited to a triangle (Fig. 2f).

2.2 General equations with restricted evaporation

We now examine the case where the evaporation rate is lower than its maximum possible rate. In the Turc space, under non-steady-state conditions ($\Delta S \leq 0$ in Fig. 2c or $\Delta S \geq 0$ in Fig. 2e), Eq. (1) should be transformed to take into account the impact of water storage on the evaporation process. We search a mathematical formulation which transforms the upper and lower limits for the steady-state conditions (Fig. 2a) into the corresponding ones for the non-steady-state conditions (Fig. 2c if $\Delta S \leq 0$ and Fig. 2e if $\Delta S \geq 0$). The mathematical transformation is searched under the form $E / E_\mathrm{p} = \alpha\ B_2(\Phi^{-1} + \gamma) + \beta$, which combines an x axis translation (γ), a y axis translation (β) and a homothetic transformation (α). This mathematical form is suggested by the way the physical domain of Turc's space is transformed when passing from steady-state conditions to non-steady-state conditions (Fig. 2a, c, e). Note that the reasoning can be conducted either in the Turc or the Budyko space, but the upper and lower limits and the transformation from steady- to non-steady-state conditions are easier to grasp in the Turc space than in the Budyko space. We distinguish the two cases corresponding to $\Delta S \leq 0$ and $\Delta S \geq 0$.

2.2.1 Case $\Delta S \leq 0$

In the Turc space, the lower limit $B_2(\Phi^{-1}) = 0$ in Fig. 2a transforms into $B_2(\Phi^{-1}) = H_\mathrm{E}$ in Fig. 2c. Using the mathematical transformation described above, we obtain $(\alpha \times 0) + \beta = H_\mathrm{E}$. Following a similar reasoning, the energy limit $B_2(\Phi^{-1}) = 1$ transforms into $B_2(\Phi^{-1}) = 1$, which yields $\alpha + \beta = 1$, and the water limit $B_2(\Phi^{-1}) = \Phi^{-1}$ transforms into $B_2(\Phi^{-1}) = H_\mathrm{E} + \Phi^{-1}$, which yields $\alpha\ (\Phi^{-1} + \gamma) + \beta = H_\mathrm{E} + \Phi^{-1}$. The resolution of these three equations gives $\alpha = 1 - H_\mathrm{E}$, $\beta = H_\mathrm{E}$ and $\gamma = \Phi^{-1} H_\mathrm{E} / (1 - H_\mathrm{E})$. Consequently, Eq. (1) should be transformed into

$$\frac{E}{E_\mathrm{p}} = (1 - H_\mathrm{E})\, B_2\left(\frac{\Phi^{-1}}{1 - H_\mathrm{E}}\right) + H_\mathrm{E}. \tag{8}$$

By introducing Eq. (1) into Eq. (8), we obtain the formulation in the Budyko space (Fig. 2d):

$$\frac{E}{P} = (1 - H_\mathrm{E})\, \Phi B_2\left(\frac{\Phi^{-1}}{1 - H_\mathrm{E}}\right) + H_\mathrm{E}\Phi = B_1\left[(1 - H_\mathrm{E})\, \Phi\right] + H_\mathrm{E}\Phi. \tag{9}$$

The derivative of Eq. (9) is

$$\frac{d\left(\frac{E}{P}\right)}{d\Phi} = (1 - H_\mathrm{E})\, \frac{dB_1\left[(1 - H_\mathrm{E})\, \Phi\right]}{d\Phi} + H_\mathrm{E}. \tag{10}$$

Given that $\frac{dB_1[(1-H_\mathrm{E})\Phi]}{d\Phi} = 1$ for $\Phi = 0$ and $\frac{dB_1[(1-H_\mathrm{E})\Phi]}{d\Phi} = 0$ when $\Phi \to \infty$, the derivative $\frac{d\left(\frac{E}{P}\right)}{d\Phi}$ (i.e., the slope of the curve) is equal to 1 for $\Phi = 0$, and when $\Phi \to \infty$, the derivative tends to H_E.

2.2.2 Case $\Delta S \geq 0$

Following the same reasoning as above, the lower limit, the energy limit and the water limit of $B_2(\Phi^{-1})$ in the Turc space in Fig. 2a (respectively, 0, 1 and Φ^{-1}) transform, respectively, into 0, 1, and $H_\mathrm{E} + \Phi^{-1}$ in Fig. 2e. We obtain, respectively, the following three equations: $(\alpha \times 0) + \beta = 0$, $\alpha + \beta = 1$ and $\alpha\ (\Phi^{-1} + \gamma) + \beta = H_\mathrm{E} + \Phi^{-1}$. The resolution gives $\alpha = 1$, $\beta = 0$ and $\gamma = H_\mathrm{E}$. Consequently, Eq. (1) should be transformed into

$$\frac{E}{E_\mathrm{p}} = B_2\left(\Phi^{-1} + H_\mathrm{E}\right). \tag{11}$$

By introducing Eq. (1) into Eq. (11), we obtain the formulation in the Budyko space (Fig. 2f):

$$\frac{E}{P} = \Phi B_2\left(\Phi^{-1} + H_\mathrm{E}\right) = (1 + H_\mathrm{E}\Phi)\, B_1\left(\frac{\Phi}{1 + H_\mathrm{E}\Phi}\right). \tag{12}$$

The derivative of Eq. (12) is

$$\frac{d\left(\frac{E}{P}\right)}{d\Phi} = H_\mathrm{E} B_1\left(\frac{\Phi}{1 + H_\mathrm{E}\Phi}\right) + (1 + H_\mathrm{E}\Phi)\, \frac{d\left[B_1\left(\frac{\Phi}{1+H_\mathrm{E}\Phi}\right)\right]}{d\Phi}. \tag{13}$$

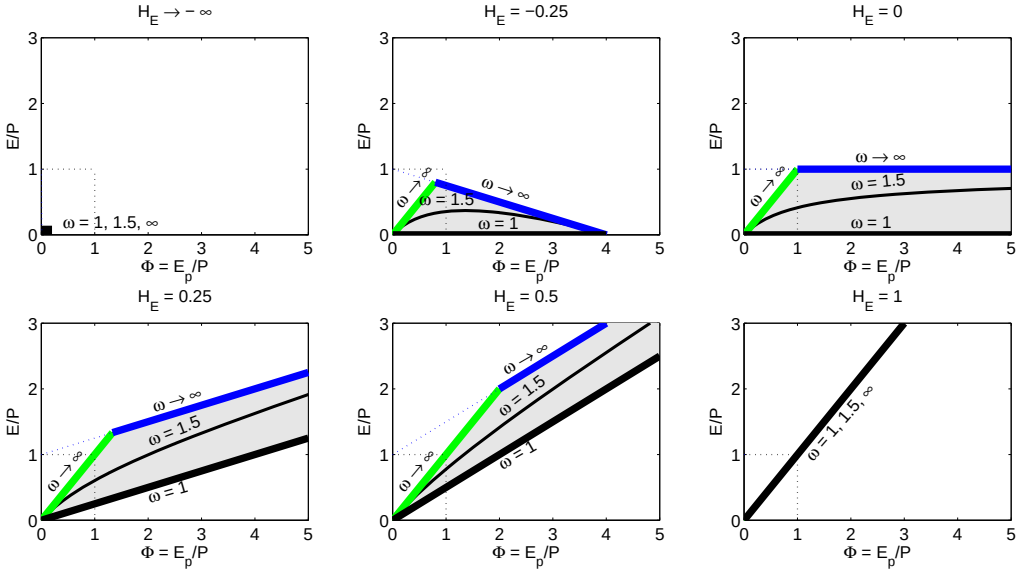

Figure 3. The ML formulation in the Budyko space with the Fu–Zhang relationship Eq. (14a, b) for $\omega = 1.5$ and for different values of H_E. The bold lines indicate the upper and lower limits of the feasible domain of evaporation (shown in grey).

Given that $B_1\left(\frac{\Phi}{1+H_E\Phi}\right) = 0$ and $\frac{d\left[B_1\left(\frac{\Phi}{1+H_E\Phi}\right)\right]}{d\Phi} = 1$ for $\Phi = 0$, the derivative $\frac{d\left(\frac{E}{P}\right)}{d\Phi}$ is equal to 1 for $\Phi = 0$. When $\Phi \to -1/H_E$, $B_1\left(\frac{\Phi}{1+H_E\Phi}\right) = 1$ and $\frac{d\left[B_1\left(\frac{\Phi}{1+H_E\Phi}\right)\right]}{d\Phi} = 0$, the derivative $\frac{d\left(\frac{E}{P}\right)}{d\Phi}$ tends to H_E.

In the following, these new generic formulae (Eqs. 8 and 9 for $\Delta S \le 0$ and Eqs. 11 and 12 for $\Delta S \ge 0$) are called ML formulations (ML stands for Moussa–Lhomme).

2.2.3 Application

Any Budyko equation $B_1(\Phi)$ from Table 1 can be used in Eqs. (9) and (12) as detailed in Table S1 in the Supplement. It is worth noting that both the Turc–Mezentsev and Fu–Zhang functions, which are obtained from the resolution of a Pfaffian differential equation, have the following remarkable simple property: $F(1/x) = F(x)/x$. This means that the same mathematical expression is valid for B_1 and B_2: $B_1 = B_2$. Both Turc–Mezentsev and Fu–Zhang functions have similar shapes, and a simple linear relationship was established by Yang et al. (2008) between their parameters (see Table 1): $\omega = \lambda + 0.72$. The ML formulation is used hereafter with the Fu–Zhang function (Table 1) for comparison with the analytical solution of Greve et al. (2016) based upon the same function. Replacing B_1 by Fu–Zhang's equation, in Eq. (9) for $\Delta S \le 0$ and in Eq. (12) for $\Delta S \ge 0$, in the Budyko space, gives

$$\text{if } \Delta S \le 0 \text{ then } \frac{E}{P} = 1 + \Phi - \left[1 + (1 - H_E)^{\omega}\Phi^{\omega}\right]^{\frac{1}{\omega}}, \quad (14a)$$

$$\text{if } \Delta S \ge 0 \text{ then } \frac{E}{P} = 1 + (1 + H_E)\,\Phi - \left[(1 + H_E\Phi)^{\omega} + \Phi^{\omega}\right]^{\frac{1}{\omega}}. \quad (14b)$$

For $\Phi = 0$, and in both cases $\Delta S \le 0$ and $\Delta S \ge 0$, we have $E/P = 0$. However, the upper limits of Φ differ: for $\Delta S \le 0$, when $\Phi \to \infty$, $E/P \to \infty$, while for $\Delta S \ge 0$ the maximum value of Φ is $-1/H_E$ and corresponds to $E/P = 0$. Figure 3 shows some examples of the shape of the ML formulation in the Budyko space (Eq. 14a, b) for $\omega = 1.5$ and different values of H_E. Note that for the particular and unlikely case when $H_E \to -\infty$, upper and lower limits are reduced to the point ($E_p/P = 0$, $E/P = 0$). For $H_E = 0$, we obtain the curves corresponding to steady-state conditions, while for $H_E = 1$, upper and lower limits are superimposed, and the domain is restricted to the 1 : 1 line. We can easily verify that all functions in Table S1 of the Supplement give similar results.

2.3 The ML formulation in the space $[E_p/(P - \Delta S), E/(P - \Delta S)]$

As mentioned in the introduction, some authors (Chen et al., 2013; Du et al., 2016) have dealt with the non-steady conditions by modifying the Budyko reference space and replacing the precipitation P by $P - \Delta S$. Hereafter, we develop the ML formulations in this new space. The upper limits of the ML formulations can be obtained by transforming Eqs. (5) and (6) defined in the Budyko space. We get, respectively,

$$\text{if } \frac{E_p}{P - \Delta S} \ge 1 \text{ then } \frac{E_x}{P - \Delta S} = 1, \quad (15)$$

$$\text{if } \frac{E_p}{P - \Delta S} < 1 \text{ then } \frac{E_x}{P - \Delta S} = \frac{E_p}{P - \Delta S}. \quad (16)$$

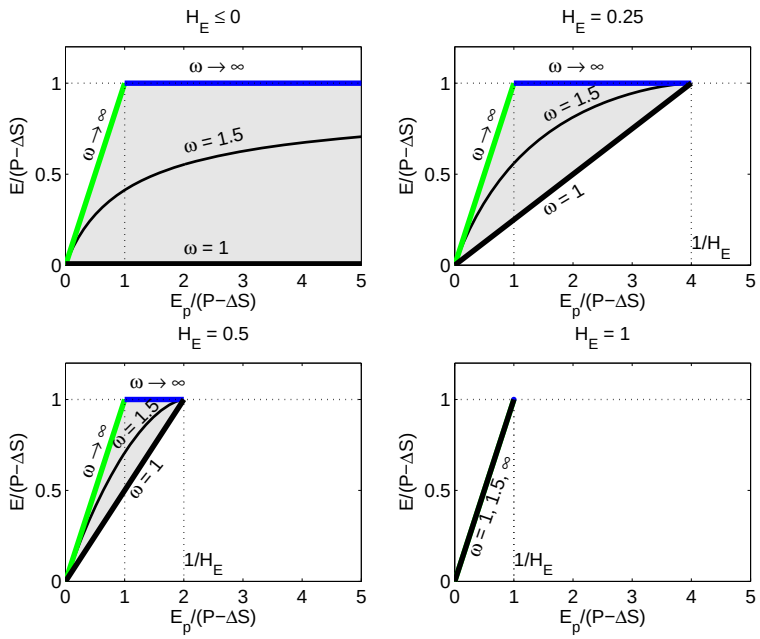

Figure 4. The ML formulation with the Fu–Zhang Eq. (21a, b) in the space $[E_\mathrm{p}\,/\,(P-\Delta S),\ E\,/\,(P-\Delta S)]$ for $\omega=1.5$ and four values of H_E. For $H_\mathrm{E}\geq 0$, all curves have a common upper end at $\Phi'=1\,/\,H_\mathrm{E}$ corresponding to $E\,/\,(P-\Delta S)=1$. The bold lines indicate the upper and lower limits of the feasible domain shown in grey. For $H_\mathrm{E}\leq 0$, the curve is similar to the one under steady-state conditions.

The lower limits are obtained from Eq. (7a, b):

$$\text{if } \Delta S \leq 0 \text{ then } \frac{E_n}{P-\Delta S}=\frac{-\Delta S}{P-\Delta S}=H_\mathrm{E}\frac{E_\mathrm{p}}{P-\Delta S}, \tag{17a}$$

$$\text{if } \Delta S \geq 0 \text{ then } \frac{E_n}{P-\Delta S}=0. \tag{17b}$$

In the new space, we put

$$\Phi'=\frac{E_\mathrm{p}}{P-\Delta S}=\frac{\Phi}{1+H_\mathrm{E}\Phi} \text{ or } \Phi=\frac{\Phi'}{1-H_\mathrm{E}\Phi'}. \tag{18}$$

Consequently, the relationship between $E\,/\,(P-\Delta S)$, Φ' and $E\,/\,P$ is given by

$$\frac{E}{P-\Delta S}=\frac{E}{P}\frac{P}{P-\Delta S}=\frac{1}{1+H_\mathrm{E}\Phi}\frac{E}{P}=\left(1-H_\mathrm{E}\Phi'\right)\frac{E}{P}. \tag{19}$$

Inserting Eqs. (9) and (12) into Eq. (19) and expressing Φ as a function of Φ' (Eq. 18) led to the ML formulation in the new space:

$$\begin{aligned}\text{if } \Delta S \leq 0 \text{ then } &\frac{E}{P-\Delta S}\\ &=\frac{1}{1+H_\mathrm{E}\Phi}\left\{B_1\left[(1-H_\mathrm{E})\,\Phi\right]+H_\mathrm{E}\Phi\right\}\\ &=\left(1-H_\mathrm{E}\Phi'\right)B_1\left[\frac{(1-H_\mathrm{E})\,\Phi'}{1-H_\mathrm{E}\Phi'}\right]+H_\mathrm{E}\Phi',\end{aligned} \tag{20a}$$

$$\begin{aligned}\text{if } \Delta S \geq 0 \text{ then } &\frac{E}{P-\Delta S}=\frac{1}{1+H_\mathrm{E}\Phi}\left(1+H_\mathrm{E}\Phi\right)\\ &\cdot B_1\left(\frac{\Phi}{1+H_\mathrm{E}\Phi}\right)=B_1\left(\Phi'\right).\end{aligned} \tag{20b}$$

Note that for $\Delta S\geq 0$, $E\,/\,(P-\Delta S)=B_1(\Phi')$ is independent of H_E and is identical to the steady-state condition $H_\mathrm{E}=0$. This is explained by the fact that the stored water ΔS being initially subtracted to the precipitation P, it does not participate in the evaporation process and consequently has no impact on the ratio $E\,/\,(P-\Delta S)$. For $\Delta S\leq 0$, and for $\Phi=0$, i.e., $P\to\infty$, we have $\Phi'=0$, $B_1=0$ and $E\,/\,(P-\Delta S)=0$. When $\Phi\to\infty$, which corresponds to $P\to 0$, we have $\Phi'=1\,/\,H_\mathrm{E}$, $B_1=1$, and $E\,/\,(P-\Delta S)\to 1$.

Any Budyko formulation B_1 in Table 1 can be used with Eq. (20a, b), as shown in Table S2 of the Supplement. When the Fu–Zhang equation is used, Eq. (20a, b) become

$$\begin{aligned}\text{if } \Delta S \leq 0 \text{ then } &\frac{E}{P-\Delta S}=1+(1-H_\mathrm{E})\,\Phi'\\ &-\left[\left(1-H_\mathrm{E}\Phi'\right)^{\omega}+(1-H_\mathrm{E})^{\omega}\left(\Phi'\right)^{\omega}\right]^{1/\omega},\end{aligned} \tag{21a}$$

$$\text{if } \Delta S \geq 0 \text{ then } \frac{E}{P-\Delta S}=1+\Phi'-\left(1+\Phi'^{\omega}\right)^{\frac{1}{\omega}}. \tag{21b}$$

Figure 4 shows the ML formulation (Eq. 21a, b) in the space $[E_\mathrm{p}\,/\,(P-\Delta S),\ E\,/\,(P-\Delta S)]$ for $\omega=1.5$ and different values of H_E. For $H_\mathrm{E}=0$, we retrieve the original Fu–Zhang equation and when $\omega=1$, we can easily verify that Eq. (21a, b) are equal to the lower limit of the domain $E\,/\,(P-\Delta S)=H_\mathrm{E}\ E_\mathrm{p}\,/\,(P-\Delta S)$ when $\Delta S\leq 0$, and $E\,/\,(P-\Delta S)=0$ when $\Delta S\geq 0$.

2.4 The ML formulation using the dimensionless parameter H_P

A mathematical development, similar to the one of Sect. 2.1, 2.2 and 2.3, is conducted in Appendix A using the dimensionless parameter $H_P = -\Delta S / P = H_E \Phi$ (instead of $H_E = -\Delta S / E_P$) and yields another form of the ML formulation. Equivalent mathematical representations are obtained for $\Delta S \leq 0$ and $\Delta S \geq 0$ in the different spaces explored in Sect. 2.1, 2.2 and 2.3. Figures S1, S2 and S3 in the Supplement obtained with the parameter H_P correspond, respectively, to Figs. 2, 3 and 4 obtained with H_E. Similarly, Tables S3 and S4 in the Supplement (obtained with H_P) correspond to Tables S1 and S2 in the Supplement (obtained with H_E): they give the ML formulation applied to the different Budyko curves of Table 1 in the standard Budyko space (E_p / P, E / P) and in the space [$E_p / (P - \Delta S)$, $E / (P - \Delta S)$]. Significant differences appear concerning the mathematical equations and the shape of the feasible domain defined by its upper and lower limits. This is due to the fact that using H_E or H_P corresponds to different sets of data and different functional representations. Both approaches (H_E or H_P) can be used. When storage water contributes to enhancing evaporation ($\Delta S \leq 0$), ΔS is bounded by potential evaporation E_P and consequently represents a given percentage of E_P. Hence, it is more convenient to use $H_E = -\Delta S / E_p$ instead of $H_P = -\Delta S / P$, because H_E lies in the range [0, 1] which is not the case for H_P. Conversely, when precipitation water contributes to increase soil water storage ($\Delta S \geq 0$), ΔS is bounded by P and represents a percentage of precipitation P. Consequently, using H_P is more convenient because H_P lies in the range $[-1, 0]$. Moreover, in order to keep the parameter in the range [0, 1], $H'_P = -H_P$ could be preferred.

3 Comparing the new formulation with other formulae from the literature

3.1 In the standard Budyko space (E_p / P, E / P)

When evapotranspiration exceeds precipitation (corresponding herein to the case $\Delta S \leq 0$), Greve et al. (2016) analytically developed a Budyko-type equation where the water storage is taken into account through a parameter y_0 ($0 \leq y_0 \leq 1$) introduced into the Fu–Zhang formulation (Table 2). In the Budyko space, this equation is written (Greve et al., 2016; Eq. 9) as

$$\frac{E}{P} = 1 + \Phi - \left[1 + (1 - y_0)^{\kappa - 1} \Phi^{\kappa}\right]^{1/\kappa}. \quad (22)$$

They used the shape parameter κ to avoid confusion with the traditional ω of Fu–Zhang equation. Despite different physical and mathematical backgrounds, Eqs. (14a) and (22) are exactly identical and a simple relationship between H_E and y_0 can be easily obtained. Equating Eqs. (14a) and (22) with

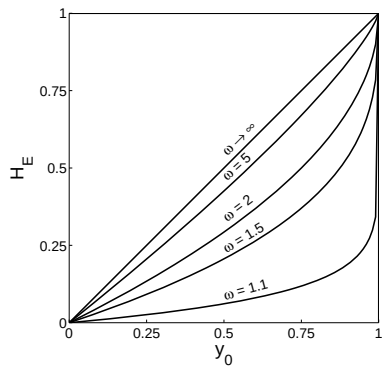

Figure 5. Relationship (Eq. 23) between the parameter H_E of the ML formulation (Eq. 14a) and the parameter y_0 of the Greve et al. (2016) (Eq. 22) for different values of ω with $\omega = \kappa$.

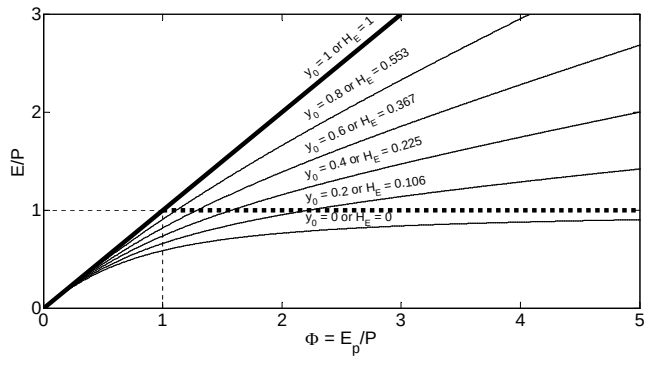

Figure 6. Example showing the similarity of the ML formulation Eq. (14a) and the equation of Greve et al. (2016) Eq. (22) (with $\omega = \kappa = 2$) for different values of y_0; the corresponding values of H_E are calculated using Eq. (23).

$\omega = \kappa$ yields

$$H_E = 1 - (1 - y_0)^{\frac{\omega - 1}{\omega}}. \quad (23)$$

The relationship between y_0 and H_E is independent from Φ. It is shown in Fig. 5 for different values of ω. For a given value of ω, we have $H_E < y_0$. For $\omega = 1$, we have $H_E = 0$, and when $\omega \to \infty$, we have $H_E = y_0$.

The derivative of Eq. (22) gives

$$\frac{d\left(\frac{E}{P}\right)}{d\Phi} = 1 - (1 - y_0)^{\kappa - 1} \Phi^{\kappa - 1} \left[1 + (1 - y_0)^{\kappa - 1} \Phi^{\kappa}\right]^{\frac{1 - \kappa}{\kappa}}. \quad (24)$$

For $\Phi = 0$, the derivative is equal to 1, and when $\Phi \to \infty$, the derivative tends to a value noted as m by Greve et al. (2016; Eq. 12):

$$m = 1 - (1 - y_0)^{\frac{\kappa - 1}{\kappa}}. \quad (25)$$

The value of the derivative (slope of the curve) is the same in both ML and Greve et al.'s (2016) formulations: for $\Phi = 0$ the derivative is equal to 1, and when $\Phi \to \infty$ we have $m = H_E$

(assuming $\omega = \kappa$). Greve et al. (2016; Sect. 4) show that y_0 is the maximum value of m reached when $\omega \to \infty$. Hence, substituting in Eq. (22) y_0 by its value inferred from Eq. (23) yields an equation identical to that obtained from the ML formulation (Eq. 14a).

Figure 6 compares the ML formulation Eq. (14a) with Greve et al.'s (2016) analytical solution Eq. (22) for $\omega = \kappa = 2$ and different values of y_0 (0, 0.2, 0.4, 0.6, 0.8 and 1). The corresponding values of H_E (respectively, 0, 0.106, 0.225, 0.367, 0.553 and 1) are calculated using Eq. (23). The new ML formulation with $\omega = \kappa$, and only for $\Delta S \leq 0$, gives exactly the same curves as those obtained by Greve et al. (2016). Both formulations are identical and have the same upper and lower limits. Greve et al. (2016), however, did not mention the lower limit and limited the reasoning to positive values of y_0. Moreover, the case of $\Delta S \geq 0$ is not considered by Greve et al. (2016).

3.2 In the space $[E_p / (P - \Delta S), E / (P - \Delta S)]$

The formulations proposed by Chen et al. (2013) and Du et al. (2016) in the space $[E_p / (P - \Delta S), (E / (P - \Delta S)]$ are essentially empirical. The Chen et al. (2013) function (Table 2) is derived from the Turc–Mezentsev equation and written as

$$\frac{E}{P - \Delta S} = \left[1 + \left(\frac{E_p}{P - \Delta S} - \Phi_t\right)^{-\lambda}\right]^{-\frac{1}{\lambda}}. \quad (26)$$

An additional parameter Φ_t is empirically introduced in order "to characterize the possible non-zero lower bound of the seasonal aridity index"; this parameter causes a shift of the curve $E / (P - \Delta S)$ along the horizontal axis such as for $E_p / (P - \Delta S) = \Phi_t$, we have $E / (P - \Delta S) = 0$. The derivative of Eq. (26) when $E_p / (P - \Delta S) \to \infty$ is equal to 0. Similarly, the Du et al. (2016) function (Table 2) is an empirical modification of Fu–Zhang equation (Fu, 1981; Zhang et al., 2004) written as

$$\frac{E}{P - \Delta S} = 1 + \frac{E_p}{P - \Delta S} - \left[1 + \left(\frac{E_p}{P - \Delta S}\right)^{\omega} + \mu\right]^{\frac{1}{\omega}}. \quad (27)$$

A supplementary parameter, noted here as μ (> -1), is added to modify the lower bound of the aridity index $E_P / (P - \Delta S)$. The parameter μ plays a similar role as Φ_t in Eq. (26). For $\mu = 0$, Eq. (27) takes the original form of Fu–Zhang equation, $(P - \Delta S)$ replacing P. When μ becomes positive, the lower end of the curve $E / (P - \Delta S)$ shifts to the right. The function $E / (P - \Delta S)$ in Eq. (27) is equal to zero for the particular value of $E_p / (P - \Delta S) = \Phi_d$, such as

$$(1 + \Phi_d)^{\omega} = 1 + (\Phi_d)^{\omega} + \mu. \quad (28)$$

Greve et al.'s (2016) formulation can be also written in the space $[E_p / (P - \Delta S), E / (P - \Delta S)]$. Inserting Eq. (22) into Eq. (20a) and expressing Φ as a function of Φ' (Eq. 18) leads

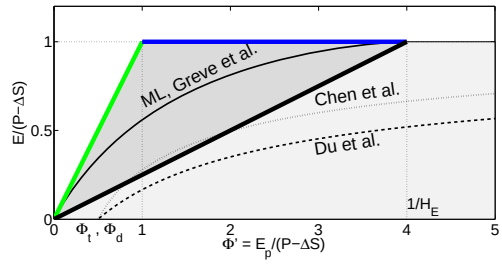

Figure 7. In the space $[E_p / (P - \Delta S), E / (P - \Delta S)]$, an example comparing the three formulations: Du et al. (2016) with $\omega = 1.5$ and $\Phi_d = 0.5$; Chen et al. (2013) with $\lambda = \omega - 0.72 = 0.78$ and $\Phi_t = \Phi_d = 0.5$; the ML formulation for $\Delta S \leq 0$ (Eq. 14a) with $\omega = 1.5$ and $H_E = 0.25$ (identical to Greve et al. 2016 formulation). The feasible domain of the ML formulation in dark grey is superimposed over the domains of both Chen et al. (2013) and Du et al. (2016) in light grey.

to

$$\frac{E}{P - \Delta S} = 1 + (1 - H_E)\,\Phi' - \left[\left(1 - H_E \Phi'\right)^{\kappa} + (1 - y_0)^{\kappa - 1}\left(\Phi'\right)^{\kappa}\right]^{1/\kappa}. \quad (29)$$

It can be mathematically shown that expressing $(1 - y_0)$ in Eq. (29) as a function of H_E by inverting Eq. (23) (assuming $\omega = \kappa$) leads to the exact ML formulation of Eq. (21a). It is a direct consequence of the similarity of both formulations. Therefore, similar curves to those shown in Fig. 4 for the ML formulation with $H_E \geq 0$ are obtained with Greve et al.'s (2016) formulation.

For $\Delta S \geq 0$ (corresponding to $H_E \leq 0$; Fig. 4), the three formulations (Chen et al.'s, 2013, Du et al.'s 2016, and ML) have similar upper and lower limits. For $\Delta S \leq 0$, Fig. 7 shows an example of the curves obtained with Du et al.'s (2016) equation ($\omega = 1.5$) and Chen et al.'s (2013) equation with $\lambda = 0.78$ (such as $\lambda = \omega - 0.72$ from Yang et al., 2008) and with $\Phi_t = \Phi_d = 0.5$ (corresponding to $\mu = 0.484$ from Eq. 28). Both Chen et al.'s (2013) and Du et al.'s (2016) formulations are compared to the ML formulation using the Fu–Zhang Eq. (14a) with $H_E = +0.25$. The ML and Greve et al. (2016) formulations are exactly identical if $\kappa = \omega = 1.5$ and $y_0 = 0.578$ calculated from Eq. (23) for $H_E = +0.25$. The four formulations have similar upper limits but the lower limits are different. Both Chen et al.'s (2013) and Du et al.'s (2016) formulations have the x axis as the lower limit and $E / (P - \Delta S)$ tends to 1 when $\Phi' = E_p / (P - \Delta S) \to \infty$, while in the ML formulation with $\Delta S \leq 0$ (Fig. 2a) the feasible domain is a triangle, the domain of variation of Φ' being limited by 0 and $1 / H_E$.

3.3 Discussion

All four formulations (ML; Greve et al., 2016; Chen et al., 2013; and Du et al., 2016) have two parameters each: one for

the shape of the curve and another for its shift due to non-steady conditions: ω and H_E for the ML formulation (with the Fu–Zhang function), κ and y_0 for Greve et al. (2016), λ and Φ_t for Chen et al. (2013), ω and μ for Du et al. (2016). If $H_E = y_0 = \Phi_t = \mu = 0$, the four formulations are identical. For $\Delta S \leq 0$, the ML formulation with the Fu–Zhang equation (Eq. 14a) is identical to the one of Greve et al. (2016) in the Budyko space and also in the $[E_p / (P - \Delta S), E / (P - \Delta S)]$ space, provided the shape parameters are assumed to be identical ($\omega = \kappa$) (a simple relationship is established between H_E and the corresponding parameter y_0). Despite similar upper limits, the ML and Greve et al. (2016) formulations behave very differently from those of Chen et al. (2013) and Du et al. (2016) in the space $[E_p / (P - \Delta S), E / (P - \Delta S)]$. The ML formulation is different for $\Delta S \leq 0$ and $\Delta S \geq 0$, while those of Chen et al.'s (2013) and Du et al.'s (2016) do not distinguish the two cases $\Delta S \leq 0$ and $\Delta S \geq 0$. All the formulations have the same upper limits, but the domain of variation of Φ' differs: respectively, $[0, 1 / H_E]$ when $\Delta S \leq 0$ and $[0, \infty]$ when $\Delta S \geq 0$ for the ML formulation, $[\Phi_t, \infty]$ for Chen et al. (2013) and $[\Phi_d, \infty]$ for Du et al. (2016) The lower end of the curve $E / (P - \Delta S)$ corresponds, respectively, to (0, 0), $(\Phi_t, 0)$ and $(\Phi_d, 0)$ and the upper end to $(1 / H_E, 1)$ when $\Delta S \leq 0$ and $(\infty, 1)$ when $\Delta S \geq 0$ for the ML formulation, $(\infty, 1)$ for the other two. Moreover, the ML formulation for $\Delta S \geq 0$ is reduced to a simple relationship $E / (P - \Delta S) = B_1 (\Phi')$ and is independent of H_E.

It is worth noting that for $\Delta S \leq 0$ the limits of Chen et al. (2013) and Du et al. (2016) functions are not completely sound from a strict physical standpoint: for very high precipitation, when $P \gg E_p$, Φ and Φ' should logically tend to zero and not to Φ_t and Φ_d; similarly, when $P \to 0$, i.e., $\Phi \to \infty$, it is physically logical that $\Phi' \to E_p / (-\Delta S) = 1 / H_E$, as predicted by our Eq. (20a). This tends to prove that the ML formulation, corroborated by the Greve et al. (2016) formulation, is physically more correct. Additionally, at simple glimpse, we note that the ML curves could be easily adjusted to the set of experimental points shown in Chen et al. (2013; Figs. 2 and 9) and in Du et al. (2016; Figs. 8 and 9).

4 Conclusion

The ML formulations constitute a general mathematical framework which allows any standard Budyko function developed at catchment scale under steady-state conditions (Table 1) to be extended to non-steady conditions (Table S1 in the Supplement). They take into account the change in catchment water storage ΔS through a dimensionless parameter $H_E = -\Delta S / E_p$ and the formulation differs according to the sign of ΔS (Eqs. 8 and 9 for $\Delta S \leq 0$ and Eqs. 11 and 12 for $\Delta S \geq 0$). Applications can be conducted at various time steps (yearly, seasonal or monthly) both in the Turc space (P / E_p, E / E_p) and in the standard Budyko space (E_p / P, E / P), with the only data required to obtain E being E_p, P and ΔS.

The new formulations are inferred from an evaluation of the feasible domain of evaporation in the Turc space, adjusted for the case where additional ($\Delta S \leq 0$) or restricted ($\Delta S \geq 0$) water is available for evaporation, and then transformed in the Budyko space. For $\Delta S = 0$, the ML formulations return the original equations under steady-state conditions, with similar upper and lower limits in both spaces. Under non-steady-state conditions, however, the upper and lower limits of the feasible domain differ when using either the Turc or the Budyko space. The ML formulations can be extended to the $[E_p / (P - \Delta S), E / (P - \Delta S)]$ space (Eq. 20a, b, Fig. 4). They can also be conducted using the dimensionless parameter $H_P = -\Delta S / P$ instead of H_E, which yields another form of the equations (Appendix A and the Supplement). It is shown that the ML formulation with $\Delta S \leq 0$ is identical to the analytical solution of Greve et al. (2016) in the standard Budyko space, a simple relationship existing between their respective parameters. On the other hand, the new formulation differs from those of Chen et al. (2013) and Du et al. (2016) in the space $[E_p / (P - \Delta S), E / (P - \Delta S)]$.

Appendix A: Scaling ΔS by P instead of E_p

Appendix A presents the set of equations when scaling the change in soil water storage ΔS by precipitation P instead of potential evaporation E_p, i.e., using $H_P = -\Delta S / P = H_E \Phi$ $(-1 \le H_P \le \Phi)$ instead of $H_E = -\Delta S / E_p$ $(-\Phi^{-1} \le H_E \le 1)$.

A1 Upper and lower limits of the Budyko framework

In the Turc space, the upper limits of evapotranspiration E_x / E_p are obtained from Eqs. (2) and (3):

$$\text{if } \frac{P}{E_p} \le 1 + \frac{\Delta S}{E_p} \text{ then } \frac{E_x}{E_p} = \frac{P}{E_p} - \frac{\Delta S}{E_p} = (1 + H_P)\,\Phi^{-1}, \tag{A1}$$

$$\text{if } \frac{P}{E_p} \ge 1 + \frac{\Delta S}{E_p} \text{ then } \frac{E_x}{E_p} = 1, \tag{A2}$$

and the lower limits of evapotranspiration E_n / E_p from Eq. (4a, b):

$$\text{if } \Delta S \le 0 \text{ then } \frac{E_n}{E_p} = -\frac{\Delta S}{E_p} = H_P \Phi^{-1}, \tag{A3a}$$

$$\text{if } \Delta S \ge 0 \text{ then } \frac{E_n}{E_p} = 0. \tag{A3b}$$

The translation in the Budyko space yields the following for the upper limits:

$$\text{if } \frac{E_p}{P} \ge \frac{E_p}{E_p + \Delta S} \text{ then } \frac{E_x}{P} = 1 - \frac{\Delta S}{P} = 1 + H_P, \tag{A4}$$

$$\text{if } \frac{E_p}{P} \le \frac{E_p}{E_p + \Delta S} \text{ then } \frac{E_x}{P} = \frac{E_p}{P} = \Phi, \tag{A5}$$

and the following for the lower limits:

$$\text{if } \Delta S \le 0 \text{ then } \frac{E_n}{P} = -\frac{\Delta S}{P} = H_E \frac{E_p}{P} = H_E \Phi = H_P, \tag{A6a}$$

$$\text{if } \Delta S \ge 0 \text{ then } \frac{E_n}{P} = 0. \tag{A6b}$$

In the Supplement, Fig. S1 shows the upper and lower limits of the feasible domain of evaporation in the Turc and Budyko spaces, drawn with the parameter $H_P = -\Delta S / P$. Figure S1 in the Supplement corresponds to Fig. 2 obtained with $H_E = -\Delta S / E_p$.

A2 General equations with restricted evaporation

We distinguish two cases: $\Delta S \le 0$ and $\Delta S \ge 0$. Substituting H_E by H_P / Φ in Eqs. (8), (9), (11) and (12) we obtain (if $\Delta S \le 0$ in the Turc space)

$$\frac{E}{E_p} = \left(1 - H_P \Phi^{-1}\right) B_2 \left(\frac{\Phi^{-1}}{1 - H_P \Phi^{-1}}\right) + H_P \Phi^{-1}, \tag{A7}$$

then in the Budyko space

$$\frac{E}{P} = B_1 (\Phi - H_P) + H_P. \tag{A8}$$

If $\Delta S \ge 0$ in the Turc space

$$\frac{E}{E_p} = B_2 \left[(1 + H_P)\,\Phi^{-1}\right], \tag{A9}$$

then in the Budyko space

$$\frac{E}{P} = (1 + H_P)\, B_1 \left(\frac{\Phi}{1 + H_P}\right). \tag{A10}$$

Replacing B_1 by Fu–Zhang's equation, in Eq. (A8) for $\Delta S \le 0$ and in Eq. (A10) for $\Delta S \ge 0$, gives the following in the Budyko space:

$$\text{if } \Delta S \le 0 \text{ then } \frac{E}{P} = 1 + \Phi - \left[1 + (\Phi - H_P)^{\omega}\right]^{\frac{1}{\omega}}, \tag{A11a}$$

$$\text{if } \Delta S \ge 0 \text{ then } \frac{E}{P} = 1 + \Phi + H_P - \left[(1 + H_P)^{\omega} + \Phi^{\omega}\right]^{\frac{1}{\omega}}. \tag{A11b}$$

In the Supplement, Fig. S2 shows an example of the ML formulation (Eq. A11a, b) in the Budyko space obtained with the parameter $H_P = -\Delta S / P$. It corresponds to Fig. 3 obtained with $H_E = -\Delta S / E_p$. Table S3 gives the ML formulation applied to the different Budyko curves of Table 1 with the parameter H_P (Eqs. A8 and A10). It corresponds to Table S1 in the Supplement obtained with H_E.

A3 The ML formulation in the space $[E_p / (P - \Delta S), E / (P - \Delta S)]$

Equations (15), (16), (17a) and (17b) yield the following for the upper limits:

$$\text{if } \frac{E_p}{P - \Delta S} \ge 1 \text{ then } \frac{E_x}{P - \Delta S} = 1, \tag{A12}$$

$$\text{if } \frac{E_p}{P - \Delta S} \le 1 \text{ then } \frac{E_x}{P - \Delta S} = \frac{E_p}{P - \Delta S}, \tag{A13}$$

and the following for the lower limits:

$$\text{if } \Delta S \le 0 \text{ then } \frac{E_n}{P - \Delta S} = \frac{-\Delta S}{P - \Delta S} = H_E \frac{E_p}{P - \Delta S} = \frac{H_P}{H_P + 1}, \tag{A14a}$$

$$\text{if } \Delta S \ge 0 \text{ then } \frac{E_n}{P - \Delta S} = 0. \tag{A14b}$$

In the new space, $[E_p / (P - \Delta S), E / (P - \Delta S)]$, we put

$$\Phi' = \frac{E_p}{P - \Delta S} = \frac{\Phi}{1 + H_P} \text{ or } \Phi = (1 + H_P)\,\Phi'. \tag{A15}$$

Consequently, the relationship between $E / (P - \Delta S)$ and E / P is given by

$$\frac{E}{P - \Delta S} = \frac{E}{P} \frac{P}{P - \Delta S} = \frac{1}{1 + H_p} \frac{E}{P}. \tag{A16}$$

Replacing H_E by H_P / Φ in Eq. (20a, b) we obtain

$$\text{if } \Delta S \leq 0 \text{ then } \frac{E}{P-\Delta S} = \frac{1}{1+H_P}\left[B_1\left(\Phi - H_P\right) + H_P\right]$$
$$= \frac{1}{1+H_P} B_1\left[\left(1+H_P\right)\Phi' - H_P\right] + \frac{H_P}{1+H_P}, \quad \text{(A17a)}$$

$$\text{if } \Delta S \geq 0 \text{ then } \frac{E}{P-\Delta S} = \left(\frac{1}{1+H_P}\right)$$
$$\cdot \left(1+H_P\right) B_1\left(\frac{\Phi}{1+H_P}\right) = B_1\left(\Phi'\right). \quad \text{(A17b)}$$

Using the Fu–Zhang equation for B_1 we get

$$\text{if } \Delta S \leq 0 \text{ then } \frac{E}{P-\Delta S} = 1 + \Phi' - \frac{H_P}{1+H_P}$$
$$-\left[\left(\frac{1}{1+H_P}\right)^{\omega} + \left(\Phi' - \frac{H_P}{1+H_P}\right)^{\omega}\right]^{1/\omega}, \quad \text{(A18a)}$$

$$\text{if } \Delta S \geq 0 \text{ then } \frac{E}{P-\Delta S} = 1 + \Phi' - \left(1+\Phi'^{\omega}\right)^{\frac{1}{\omega}}. \quad \text{(A18b)}$$

In the Supplement, Fig. S3 shows an example of the ML formulation (Eq. A18a, b) in the space $[E_p / (P-\Delta S), E / (P-\Delta S)]$ obtained with the parameter $H_P = -\Delta S / P$. It corresponds to Fig. 4 obtained with $H_E = -\Delta S / E_p$. Table S4 in the Supplement gives the ML formulation applied to the different Budyko curves of Table 1 in the space $[E_p / (P-\Delta S), E / (P-\Delta S)]$ with the parameter H_P (Eq. A17a and b). It corresponds to Table S2 in the Supplement obtained with H_E.

Appendix B: List of symbols

$B_1(\Phi)$	Relationship between E / P and Φ in the Budyko space (E_p / P, E / P) such as $E / P = B_1(\Phi)$ [–]
$B_2(\Phi^{-1})$	Relationship between E / E_p and $\Phi^{-1} = P / E_\mathrm{p}$ in the Turc space (P / E_p, E / E_p) such as $E / E_\mathrm{p} = B_2(\Phi^{-1})$ [–]
E	actual evaporation [LT^{-1}]
E_n	Lower limit of the feasible domain of evaporation [LT^{-1}]
E_p	Potential evaporation [LT^{-1}]
E_x	Upper limit of the feasible domain of evaporation [LT^{-1}]
H_E	$-\Delta S / E_\mathrm{p}$ ($-P / E_\mathrm{p} \leq H_\mathrm{E} \leq 1$) [–]
H_P	$-\Delta S / P$ ($-1 \leq H_\mathrm{P} \leq E_\mathrm{p} / P$) [–]
m	Slope of the equation of Greve et al. (2016) when $\Phi \to \infty$ [–]
ML	New formulations: Eqs. (8) and (9) for $\Delta S \leq 0$ and Eqs. (11) and (12) for $\Delta S \geq 0$ (stands for Moussa–Lhomme)
P	Precipitation [LT^{-1}]
Q	Runoff [LT^{-1}]
y_0	Parameter in the Greve et al. (2016) equation accounting for non-steady-state conditions ($0 \leq y_0 \leq 1$) [–]
κ	Shape parameter in the Greve et al. (2016) equation corresponding to ω in the Fu–Zhang equation [–]
ΔS	Water storage variation [LT^{-1}]
λ	Shape parameter in the Turc–Mezentsev equation ($\lambda > 0$) [–]
μ	Parameter in the Du et al. (2013) equation [–]
Φ	Aridity index ($\Phi = E_\mathrm{p} / P$) [–]
Φ_d	Aridity index threshold in the Du et al. (2016) equation corresponding to $E / (P - \Delta S) = 0$ [–]
Φ_t	Aridity index threshold in the Chen et al. (2013) equation [–]
Φ'	$E_\mathrm{p} / (P - \Delta S)$ [–]
ω	Shape parameter of the Fu–Zhang equation ($\omega > 1$) [–]

The Supplement related to this article is available online at doi:10.5194/hess-20-4867-2016-supplement.

Acknowledgements. The authors are very grateful to the reviewers, L. Gudmundsson and F. Jaramillo, and to the editor, M. Coenders-Gerrits, for their constructive comments of the manuscript. They also gratefully acknowledge the scientific and financial support of the UMR LISAH, as well as the always inspiring advice of A. Gaby.

Edited by: M. Coenders-Gerrits
Reviewed by: L. Gudmundsson and one anonymous referee

References

Alley, W. M.: On the treatment of evapotranspiration, soil moisture accounting, and aquifer recharge in monthly water balance models, Water Resour. Res., 20, 1137–1149, 1984.

Andréassian, V., Mander, Ü., and Pae, T.: The Budyko hypothesis before Budyko: The hydrological legacy of Evald Oldekop, J. Hydrol., 535, 386–391, doi:10.1016/j.jhydrol.2016.02.002, 2016.

Budyko, M. I.: Climate and life, Academic Press, Orlando, FL, 508 pp., 1974.

Carmona, A., Sivapalan, M., Yaeger, M. A., and Poveda, G.: Regional patterns of interannual variability of catchment water balances across the continental U.S.: A Budyko framework, Water Resour. Res., 50, 9177–9193, doi:10.1002/2014WR016013, 2014.

Chen, X., Alimohammadi, N., and Wang, D.: Modeling interannual variability of seasonal evaporation and storage change based on the extended Budyko framework, Water Resour. Res., 49, 6067–6078, doi:10.1002/wrcr.20493, 2013.

Choudhury, B.: Evaluation of an empirical equation for annual evaporation using field observations and results from a biophysical model, J. Hydrol., 216, 99–110, 1999.

Donohue, R. J., Roderick, M. L., and McVicar, T. R.: On the importance of including vegetation dynamics in Budyko's hydrological model, Hydrol. Earth Syst. Sci., 11, 983–995, doi:10.5194/hess-11-983-2007, 2007.

Du, C., Sun, F., Yu, J., Liu, X., and Chen, Y.: New interpretation of the role of water balance in an extended Budyko hypothesis in arid regions. Hydrol. Earth Syst. Sci., 20, 393–409, doi:10.5194/hess-20-393-2016, 2016.

Fang, K., Shen, C., Fisher, J. B., and Niu, J.: Improving Budyko curve-based estimates of long-term water partitioning using hydrologic signatures from GRACE, Water Resour. Res., 52, 5537–5554, doi:10.1002/2016WR018748, 2016.

Fu, B. P.: On the calculation of evaporation from land surface (in Chinese), Sci. Atmos. Sin., 5, 23–31, 1981.

Gentine, P., D'Odorico, P., Lintner, B. R., Sivandran, G., and Salvucci, G.: Interdependence of climate, soil, and vegetation as constrained by the Budyko curve, Water Resour. Res., 39, L19404, doi:10.1029/2012GL053492, 2012.

Greve, P., Gudmundsson, L., Orlowsky, B., and Seneviratne, S. I.: A two-parameter Budyko function to represent conditions under which evapotranspiration exceeds precipitation, Hydrol. Earth Syst. Sci., 20, 2195–2205, doi:10.5194/hess-20-2195-2016, 2016.

Istanbulluoglu, E., Wang, T., Wright, O. M., and Lenters, J. D.: Interpretation of hydrologic trends from a water balance perspective: The role of groundwater storage in the Budyko hypothesis, Water Resour. Res., 48, W00H16, doi:10.1029/2010WR010100, 2012.

Jaramillo, F. and Destouni, G.: Local flow regulation and irrigation raise global human water consumption and footprint, Science, 350, 1248–1250, 2015.

Li, D., Pan, M., Cong, Z., Zhang, L., and Wood, E.: Vegetation control on water and energy balance within the Budyko framework, Water Resour. Res., 49, 969–976, doi:10.1002/wrcr.20107, 2013.

Mezentsev, V.: More on the computation of total evaporation, Meteorol. Gidrol., 5, 24–26, 1955.

Oldekop, E. M.: On evaporation from the surface of river basins, Collection of the Works of Students of the Meteorological Observatory, University of Tartu-Jurjew-Dorpat, Tartu, Estonia, p. 209, 1911.

Tixeront, J.: Prediction of streamflow, IAHS publication no. 63: General Assembly of Berkeley, IAHS, Gentbrugge, 118–126, 1964.

Turc, L.: Le bilan d'eau des sols: relations entre les précipitations, l'évaporation et l'écoulement, Ann. Agron., 5, 491–595, 1954.

Wang, D.: Evaluating interannual water storage changes at watersheds in Illinois based on long-term soil moisture and groundwater level data, Water Resour. Res., 48, W03502, doi:10.1029/2011WR010759, 2012.

Wang, X.-S. and Zhou, Y.: Shift of annual water balance in the Budyko space for catchments with groundwater-dependent evapotranspiration, Hydrol. Earth Syst. Sci., 20, 3673–3690, doi:10.5194/hess-20-3673-2016, 2016.

Yang, D., Shao, W., Yeh, P. J. F., Yang, H., Kanae, S., and Oki, T.: Impact of vegetation coverage on regional water balance in the nonhumid regions of China, Water Resour. Res., 45, W00A14, doi:10.1029/2008WR006948, 2009.

Yang, H., Yang, D., Lei, Z., and Sun, F.: New analytical derivation of the mean annual water-energy balance equation, Water Resour. Res., 44, W03410, doi:10.1029/2007WR006135, 2008.

Zhang, L., Dawes, W. R., and Walker, G. R.: Response of mean annual evapotranspiration to vegetation changes at catchment scale, Water Resour. Res., 37, 701–708, 2001.

Zhang, L., Hickel, K., Dawes, W. R., Chiew, F. H. S., Western, A. W., and Briggs, P. R.: A rational function approach for estimating mean annual evapotranspiration, Water Resour. Res., 40, W02502, doi:10.1029/2003WR002710, 2004.

Zhang, L., Potter, N., Hickel, K., Zhang, Y., and Shao, Q.: Water balance modeling over variable time scales based on the Budyko framework – Model development and testing, J. Hydrol., 360, 117–131, doi:10.1016/j.jhydrol.2008.07.021, 2008.